Leukemia Research 34 (2010) 677–681

Contents lists available at ScienceDirect

Leukemia Research

journal homepage: www.elsevier.com/locate/leukres

Brief communication

Micro-RNA-15a and micro-RNA-16 expression and chromosome 13 deletions in multiple myeloma

Sophie L. Corthals[a], Mojca Jongen-Lavrencic[a], Yvonne de Knegt[a], Justine K. Peeters[a], H. Berna Beverloo[b], Henk M. Lokhorst[c], Pieter Sonneveld[a,*]

[a] Department of Hematology, Erasmus Medical Centre Rotterdam, Rotterdam, The Netherlands
[b] Department of Clinical Genetics, Erasmus Medical Centre Rotterdam, Rotterdam, The Netherlands
[c] Department of Hematology, University Medical Center Utrecht, Utrecht, The Netherlands

ARTICLE INFO

Article history:
Received 15 October 2009
Received in revised form 28 October 2009
Accepted 28 October 2009
Available online 23 December 2009

Keywords:
Multiple myeloma
Micro-RNA
Chromosome 13 deletion

ABSTRACT

We have used copy number variation (CNV) analysis with SNP mapping arrays for *miRNA-15a* and *miRNA-16-1* expression analysis in patients with multiple myeloma (MM) with or without deletion of chromosome 13q14. *MiRNA-15a* and *miRNA-16* display a range of expression patterns in MM patients, independent of the chromosome 13 status. These findings suggest that genes other than *miR-15a* and *miR-16* may explain the prognostic significance of 13q14 deletions.

1. Introduction

Multiple myeloma (MM) is a dismal disease with a median survival of 3–5 years [1].

MM is characterized by genetic instability and chromosomal translocations early in disease progression play an important role in the pathogenesis of MM. Chromosome 13 aberrations occur in 50% and the most commonly deleted marker in the 13q14 region is D13S319, located distal to the retinoblastoma-1 (*RB1*) gene [2,3]. It is now common practice to determine the presence of chromosome 13 deletions by fluorescence in situ hybridization (FISH) [4–10]. The adverse prognostic role of these deletions has been attributed to the presence of MM tumor suppressor gene(s) on chromosome 13q which as yet have not been identified.

Micro-RNAs (miRs) are a class of small non-coding single stranded RNAs of approximately 22 nucleotides in length [11]. MiRs negatively regulate gene expression by binding to partially complementary sites in messenger RNAs (mRNAs) [12]. miRs may play a role in the pathogenesis of MM [13,14]. In chronic lymphocytic leukemia (CLL), *miR-15a* and *miR-16-1* are frequently downregulated [15]. We evaluated the expression of *miR-15a* and *miR-16-1* in MM.

2. Materials and methods

We obtained bone marrow samples from newly diagnosed patients with MM. Myeloma plasma cells were purified >80% using CD138 magnetic microbeads (MACS system, Miltenyi Biotec, Bergisch Gladbach, Germany). Small RNA transcripts less than 200 nucleotides in length including miRs, were isolated from CD138 magnetic cell selected (MACS) MM plasma cells using miRVana™ miRNA Isolation Kit (Ambion, Austin, TX). RNA levels and quality were assessed using the Agilent 2100 Bioanalyzer (Agilent Technologies). Mature *miR-15a* and *miR-16* expression levels in MM plasma cells were determined by real-time PCR using TaqMan miR assay (Applied Biosystems, P/N: 4373123 and 4373121) [16]. All experiments were performed in duplicate and miRs were considered as present when C_T-values were lower than 35. Genomic DNA was isolated from peripheral blood by salting out precipitation. Tumor DNA was extracted from CD138 MACS MM plasma cells using Qiagen RNAeasy kit (Qiagen, Valencia, CA). Genome-wide SNP genotyping was performed using the Illumina Infinium HumanHap550 Genotyping BeadChip, containing over 550,000 unique tag SNP markers, according to manufacturer's instructions (Illumina, San Diego, CA).

Genotypes for all arrays were calculated using BeadStudio's genotyping module (v2.0, Illumina). Data was imported into Partek Genomics Suite 6.4 software (Partek Inc., St Louis, MO) for further analysis; allele intensities were calculated for 25 genomic DNA MM samples and 26 tumor DNA MM samples, of which 20 had paired normal samples. For these 20 samples, paired analysis was performed. Allele specific copy number variation (AsCN) was calculated by estimating the number of copies for each allele, rather than total copies of each chromosome. Loss of heterozygosity (LOH) was estimated from the imported sample genotypes by a Hidden Markov Model, using the same baseline as in the segmentation algorithm (25

* Corresponding author at: Department of Hematology, Erasmus Medical Centre Rotterdam, Room No. L439, PO Box 2040, 3000 CA Rotterdam, The Netherlands. Tel.: +31 10 7033123; fax: +31 10 7035814.
E-mail address: p.sonneveld@erasmusmc.nl (P. Sonneveld).

0145-2126/$ – see front matter © 2009 Elsevier Ltd. All rights reserved.
doi:10.1016/j.leukres.2009.10.026

Table 1
Chromosome 13 aberrations of the region flanking miR-15a and miR-16-1 identified by FISH and segmentation analysis using SNP mapping arrays.

Patient	FISH	Segmentation	Analysis type	Start	End	Cytoband	Length (bps)	Copy Number	# Markers	Genes
MM 1	Δ13	Del	Paired	42503650	57487878	13ql4.11–13q21.1	14984228	0.6930	2789	ARL11, C13orfl, DLEU1, EBPL, KCNRG, KPNA3, PHF11, RCBTB1, SETDB2, TRIM13
MM 2	Del	Del	Paired	27313597	57610331	13ql2.2–13q21.2	30296734	1.0028	6342	ARL11, C13orfl, DLEU1, EBPL, KCNRG, KPNA3, PHF11, RCBTB1, SETDB2, TRIM13
MM 3	Del	Del	Paired	47862787	114121253	13ql4.2–13q34	66258466	0.9633	13801	ARL11, C13orfl, DLEU1, EBPL, KCNRG, KPNA3, PHF11, RCBTB1, SETDB2, TRIM13
MM 4	Del	Del	Paired	45560358	52963785	13ql4.12–13q21.1	7403427	0.8485	1488	ARL11, C13orfl, DLEU1, EBPL, KCNRG, KPNA3, PHF11, RCBTB1, SETDB2, TRIM13
MM 5	Del	Del	Paired	48984705	53079298	13ql4.3–13q21.1	4094593	0.7389	828	ARL11, C13orfl, DLEU1, EBPL, KCNRG, KPNA3, PHF11, RCBTB1, SETDB2, TRIM13
MM 6	Del	Del	Paired	43781771	70193498	13ql4.11–13q21.33	26411727	0.6852	4764	ARL11, C13orfl, DLEU1, EBPL, KCNRG, KPNA3, PHF11, RCBTB1, SETDB2, TRIM13
MM 7	Del	Del	Paired	40498617	70309383	13ql4.11–13q21.33	29810766	0.5797	5616	ARL11, C13orfl, DLEU1, EBPL, KCNRG, KPNA3, PHF11, RCBTB1, SETDB2, TRIM13
MM 8	Del	Del	Paired	47786017	104600044	13ql4.2–13q33.2	56814027	1.2421	11446	ARL11, C13orfl, DLEU1, EBPL, KCNRG, KPNA3, PHF11, RCBTB1, SETDB2, TRIM13
MM 9	Del	Del	Paired	39203461	66142848	13ql3.3–13q21.32	26939387	0.9434	5040	ARL11, C13orfl, DLEU1, EBPL, KCNRG, KPNA3, PHF11, RCBTB1, SETDB2, TRIM13
MM 10	Del	Del	Paired	40531599	53088969	13ql4.11–13q21.1	12557370	0.9634	2661	ARL11, C13orfl, DLEU1, EBPL, KCNRG, KPNA3, PHF11, RCBTB1, SETDB2, TRIM13
MM 11	Del	Del	Unpaired	45324420	52963785	13ql4.12–13q21.1	7639365	0.9586	1529	ARL11, C13orfl, DLEU1, EBPL, KCNRG, KPNA3, PHF11, RCBTB1, SETDB2, TRIM13
MM 12	Del	Del	Unpaired	22372135	78494745	13ql2.12–13q31.1	56122610	1.0474	11979	ARL11, C13orfl, DLEU1, EBPL, KCNRG, KPNA3, PHF11, RCBTB1, SETDB2, TRIM13
MM 13	N	Del	Paired	49431816	49631113	13ql4.3	199297	1.0060	19	KCNRG, TRIM13
MM 14	N	Del	Paired	49024071	52210918	13ql4.3–13q21.1	3186847	1.2947	572	ARL11, C13orfl, EBPL, KCNRG, KPNA3, RCBTB1, TRIM13
MM 15	N	Del	Paired	26462920	104775995	13ql2.13–13q33.2	78313075	0.8103	16439	ARL11, C13orfl, DLEU1, EBPL, KCNRG, KPNA3, PHF11, RCBTB1, SETDB2, TRIM13
MM 16	N	Del	Paired	34866084	97736842	13ql3.3–13q32.2	62870758	1.4238	12446	ARL11, C13orfl, DLEU1, EBPL, KCNRG, KPNA3, PHF11, RCBTB1, SETDB2, TRIM13
MM 17	N	Del	Paired	49358246	49631113	13ql4.3	272867	0.5809	23	C13orfl, KCNRG, TRIM13
MM 18	N	Del	Unpaired	37338941	52972100	13ql3.3–13q21.1	15633159	1.0293	3373	ARL11, C13orfl, DLEU1, EBPL, KCNRG, KPNA3, PHF11, RCBTB1, SETDB2, TRIM13
MM 19	N	Del	Unpaired	48984705	52958855	13ql4.3–13q21.1	3974150	1.3794	796	ARL11, C13orfl, EBPL, KCNRG, KPNA3, PHF11, RCBTB1, TRIM13
MM 20	N	Del	Unpaired	48951859	68490076	13ql4.3–13q21.33	19538217	1.5462	3374	ARL11, C13orfl, DLEU1, EBPL, KCNRG, KPNA3, PHF11, RCBTB1, SETDB2, TRIM13
MM 21	N	N	Paired							
MM 22	N	N	Unpaired							
MM 23	N	N	Paired							
MM 24	N	N	Paired							
MM 25	N	N	Paired							
MM 26	N	N	Paired							

N indicates normal; Del, deletion; A13, deletion; Amp, amplification; ND, not done.

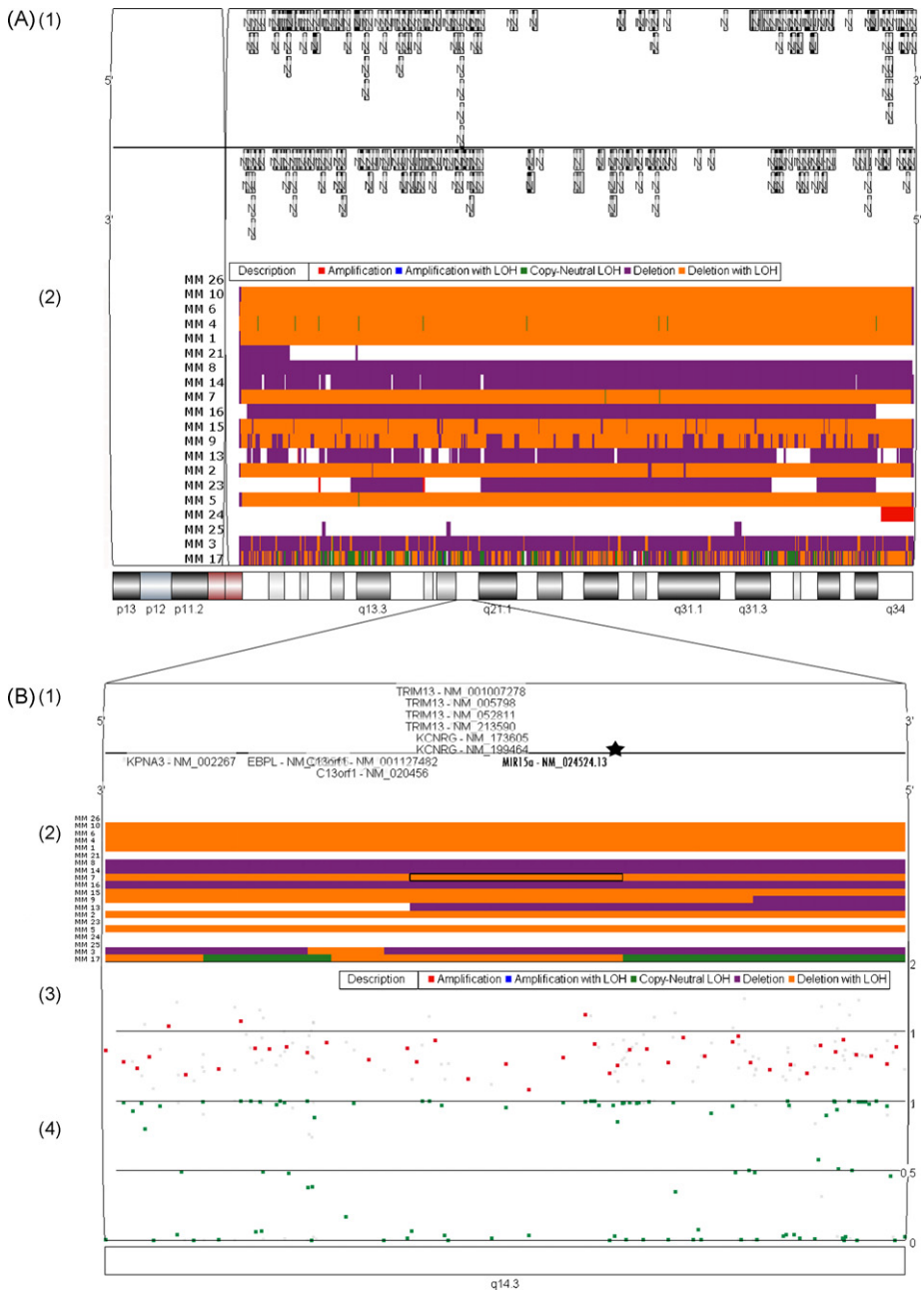

Fig. 1. Copy number alterations of chromosome 13 as determined by paired segmentation analysis. SNP mapping arrays (Illumina Infinium HumanHap550 Genotyping BeadChip) were used to determine the exact deleted regions at chromosome 13 of multiple myeloma (MM) cases. (A) In panel 1; the genome browser illustrates the gene transcripts (NCBI) located on chromosome 13. The results of the paired segmentation analysis of chromosome 13 (20/26 MM patients) are shown in the panel 2. (B) A region on chromosome 13; 13q14.3, including the *miR-15a* and *miR-16* locus, is depicted at larger magnification. In panel 1 the *miR-15a* and *miR-16* locus (star) is shown within the genome browser. Panel 2 shows the results of the paired segmentation analysis in more detail. A deletion (orange and purple) was detected in 15/20 MM patients. Uniparental disomy (UPD; green) was detected in patient MM 17, in the regions flanking *miR-15a* and *miR-16*-1. Copy number (CN) values for SNPs (red dots) are plotted in panel 3. CN values of 2 represent diploid copy number, whereas values of 1 and 0 represent heterozygous and homozygous deletion, respectively. A representative patient (MM 7) shows values of 1 or $\leq$1, indicating deletion. In panel 4 the B allele frequency is displayed. Each point (green dot) represents the B allele frequency of one SNP. B allele frequencies of 0 and 1 represent homozygous signals (AA or BB), while an allele frequency of ~0.5 represents an equal contribution from both alleles (AB). A representative MM patient sample (MM 7) shows a deletion with LOH (black box in segmentation panel) which produces a characteristic pattern that lacks heterozygote signal. For visualization purposes the order of the samples is MM 26, MM 10, MM 4, MM 1, MM 21, MM 8, MM 14, MM 7. MM 16, MM 15, MM 9, MM 13, MM 2, MM 23, MM 5, MM 24, MM 25, MM 3, and MM 17.

genomic blood DNA MM samples). CN, AsCN, LOH and allelic ratios were integrated and visualized in a genomic browser within Partek Genomics Suite.

Chromosome analysis was performed using both QFQ- and RBA-banding [17]. Fluorescence in situ hybridization (FISH) was performed using standard protocols [18].

In this study, the stability of five candidate reference small nuclear RNAs was examined using the validation program GeNorm [19]. The relative expression levels of *miR-15a* and *miR-16* compared to CD138 sorted plasma cells from normal bone marrow were determined using the $2^{-\Delta\Delta Ct}$ method [20].

The Mann–Whitney *U*-test was applied to determine differences of the *miR-15a* or *miR-16* gene expression levels.

3. Results

FISH analysis showed chromosome 13 deletions in 11/26 patients (Table 1 and Table S1). Using karyotyping, 1 additional patient had a chromosome 13 deletion, resulting in 12/26 patients (46.2%) having a chromosome 13 aberration. CNV analysis using SNP mapping arrays performed on 20/26 paired samples indicated that a minimally deleted region on chromosome 13 (49431816–49631113 bp), in which *miR-15a* and *miR-16-1* are

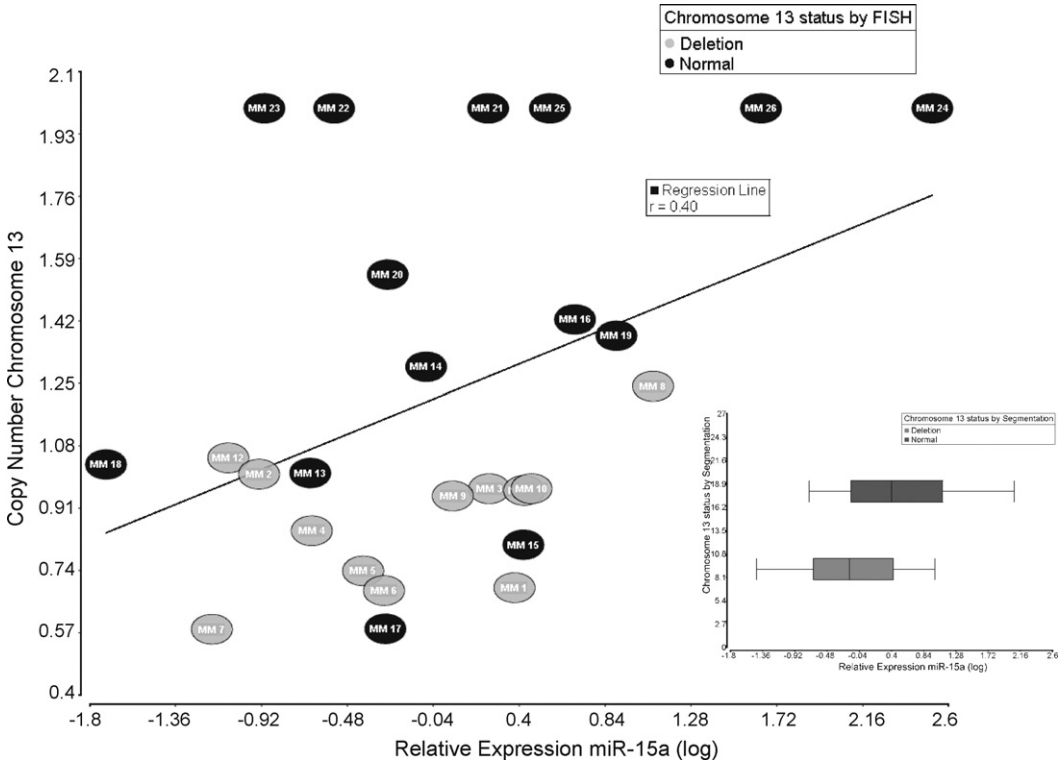

Fig. 2. Copy number of chromosome 13 in correlation with *miR-15a* gene expression in multiple myeloma (MM) patient samples. A TaqMan miR assay was used to determine the relative *miR-15a* expression levels in myeloma plasma of 26 MM patients. The normalized relative expression of *miR-15a* in 26 MM patient samples is displayed on the *X*-axis. *MiR-15a* is expressed in all 26 MM samples, although the level of expression varies across the samples. SNP mapping arrays (Illumina Infinium HumanHap550 Genotyping BeadChip) were used to determine copy number values of chromosome 13, which are shown on the *Y*-axis. Copy number values of 2 were detected in 6/26 MM patients, indicating diploid copy number. Values less than 2 represent heterozygous and homozygous deletions, which were found in 20/26 MM patients. Patients are coloured by chromosome 13 status as determined by FISH; being either normal (black) or deletion (gray). Segmentation analysis has shown 8 additional patients with a chromosome 13 aberration in the region containing *miR-15a* and *miR-16-1*. A linear regression line reveals there is no correlation between the *miR-15a* expression and the chromosome 13 status as determined by segmentation analysis. The picture insert shows a box plot representation of the normalized relative expression of *miR-15a* in 26 MM patients samples (*X*-axis), in correlation with the chromosome 13 status determined by segmentation (*Y*-axis). The box plot shows no significant difference in *miR-15a* gene expression ($P = 0.38$, Mann–Whitney *U*-test) between patients with a deletion (gray, $n = 20$) and normal chromosome 13 status (black, $n = 6$).

located, was observed in 20/26 patients, 15 of which were from the paired analysis ($P < 0.00001$) (Table 1 and Tables S1 and S2 and Fig. 1, Fig. S1). Segmentation analysis revealed 8 additional patients with a chromosome 13 deletion compared to FISH analysis. AsCN analysis further revealed the absence of homozygous deletions in these patients. No uniparental disomy (UPD; copy number-neutral LOH), was detected in the exact location of *miR-15a* and *miR-16-1* (Fig. 1 and Fig. S1). A highly correlated cluster of miRs; *miR-15b* and *miR-16-2*, is located on chromosome 3. *MiR-15a* and *miR-15b* are derived from the same seed sequence, however, they differ in their mature sequence and therefore cannot be distinguished. For this reason, we are not able to separate *miR-16-1* and *16-2* expression using the real-time PCR assay, since the mature miR sequence primes the assay. As these highly correlated miRs are located on chromosome 3, we have also examined this region. Analysis of this chromosome was performed using the segmentation algorithm to determine the amplified and deleted regions (*miR-15b* and *miR-16-2* location 161605070–161605307 bp). Deletion of this region on chromosome 3 was found in 2 MM and amplification in 6 MM patients (Table S2).

Both *miR-15a* and *miR-16* were expressed in all 26 MM samples. The median expression value of *miR-15a* and *miR-16* was 0.84 and 1.16, respectively (both values in log2 scale, relative to the geometric mean). No significant association was found between the chromosome 13 deletion status and the *miR-15a* expression levels using FISH ($P = 0.38$) and CNV ($P = 0.25$) (Fig. 2). In addition, statistical analysis showed no significant association between *miR-16* expression and chromosome 13 status by FISH ($P = 0.40$) or CNV ($P = 0.27$). We also evaluated the expression levels of *miR-15a* and *miR-16* in CD138 sorted plasma cells from normal individuals. *MiR-16* was expressed at 1.4-fold lower levels in normal plasma cells when compared with myeloma plasma cells.

These findings demonstrate that *miR-15a* and *miR-16* are displayed at a range of expression levels in MM patients which are higher than in normal plasma cell counterparts. The expression of these miRs varies independent of the chromosome 13 status.

4. Discussion

Deletion of chromosome 13 is detected in 50% of patients by FISH and in 10–20% by karyotyping [5,21–23]. Patients with a whole chromosome 13 deletion detected by cytogenetics, have a worse prognosis than 13q deletions detected by FISH [24–27]. Loss of chromosome 13 occurs, like in MM, in approximately 50% of CLL patients, although CLL patients with 13q deletions have favorable survival [28]. Differences of the length of the involved region may explain these observations [29].

Downregulation of *miR-15a* and *miR-16-1* has been reported in cases of MM, CLL and diffuse B Cell Lymphomas [14,15,30]. In this study, the two miRs were expressed in all 26 MM patients examined, even when chromosome 13 was deleted. Our analysis showed an high specificity for detecting allelic imbalances in heterogeneous samples [31,32]. It is unlikely that chromosome 13 deletions that are not detected by CNV analysis are partial deletions. Compensation by the non-deleted allele could explain the expression level

of *miR-16* since all chromosome 13 deletions in this study are heterozygous.

This study clearly shows the discrepancy between FISH and CNV analysis and the efficacy of SNP mapping arrays in detecting chromosomal aberration. It is important that a direct comparison between tumor DNA and matched germline DNA was performed [33]. Because paired CN analysis was carried out for 20/26 MM samples, this makes the data highly reliable. In conclusion, high resolution, genome-wide SNP mapping arrays may provide an excellent tool to identify partial chromosomal aberrations and genes.

Conflict of interest statement

There are no conflict of interests in relation to this work.

Appendix A. Supplementary data

Supplementary data associated with this article can be found, in the online version, at doi:10.1016/j.leukres.2009.10.026.

References

[1] Kyle RA, Rajkumar SV. Multiple myeloma. N Engl J Med 2004;351(18):1860–73.
[2] Avet-Louseau H, Daviet A, Sauner S, Bataille R. Chromosome 13 abnormalities in multiple myeloma are mostly monosomy 13. Br J Haematol 2000;111(4):1116–7.
[3] Shaughnessy J, Tian E, Sawyer J, Bumm K, Landes R, Badros A, et al. High incidence of chromosome 13 deletion in multiple myeloma detected by multiprobe interphase FISH. Blood 2000;96(4):1505–11.
[4] Debes-Marun CS, Dewald GW, Bryant S, Picken E, Santana-Davila R, Gonzalez-Paz N, et al. Chromosome abnormalities clustering and its implications for pathogenesis and prognosis in myeloma. Leukemia 2003;17(2):427–36.
[5] Facon T, Avet-Loiseau H, Guillerm G, Moreau P, Genevieve F, Zandecki M, et al. Chromosome 13 abnormalities identified by FISH analysis and serum beta2-microglobulin produce a powerful myeloma staging system for patients receiving high-dose therapy. Blood 2001;97(6):1566–71.
[6] Fonseca R, Harrington D, Oken MM, Dewald GW, Bailey RJ, Van Wier SA, et al. Biological and prognostic significance of interphase fluorescence in situ hybridization detection of chromosome 13 abnormalities (delta13) in multiple myeloma: an eastern cooperative oncology group study. Cancer Res 2002;62(3):715–20.
[7] Seong C, Delasalle K, Hayes K, Weber D, Dimopoulos M, Swantkowski J, et al. Prognostic value of cytogenetics in multiple myeloma. Br J Haematol 1998;101(1):189–94.
[8] Shaughnessy J, Barlogie B. Chromosome 13 deletion in myeloma. Curr Top Microbiol Immunol 1999;246:199–203.
[9] Tricot G, Barlogie B, Jagannath S, Bracy D, Mattox S, Vesole DH, et al. Poor prognosis in multiple myeloma is associated only with partial or complete deletions of chromosome 13 or abnormalities involving 11q and not with other karyotype abnormalities. Blood 1995;86(11):4250–6.
[10] Zojer N, Konigsberg R, Ackermann J, Fritz E, Dallinger S, Kromer E, et al. Deletion of 13q14 remains an independent adverse prognostic variable in multiple myeloma despite its frequent detection by interphase fluorescence in situ hybridization. Blood 2000;95(6):1925–30.
[11] Griffiths-Jones S, Grocock RJ, van Dongen S, Bateman A, Enright AJ. miRBase: microRNA sequences, targets and gene nomenclature. Nucleic Acids Res 2006;34:D140–4 [Database issue].
[12] Bartel DP. MicroRNAs: genomics, biogenesis, mechanism, and function. Cell 2004;116(2):281–97.
[13] Pichiorri F, Suh SS, Ladetto M, Kuehl M, Palumbo T, Drandi D, et al. MicroRNAs regulate critical genes associated with multiple myeloma pathogenesis. Proc Natl Acad Sci USA 2008;105(35):12885–90.
[14] Roccaro AM, Sacco A, Thompson B, Leleu X, Azab AK, Azab F, et al. microRNAs 15a and 16 regulate tumor proliferation in multiple myeloma. Blood 2009.
[15] Calin GA, Dumitru CD, Shimizu M, Bichi R, Zupo S, Noch E, et al. Frequent deletions and down-regulation of micro-RNA genes miR15 and miR16 at 13q14 in chronic lymphocytic leukemia. Proc Natl Acad Sci USA 2002;99(24):15524–9.
[16] Chen C, Ridzon DA, Broomer AJ, Zhou Z, Lee DH, Nguyen JT, et al. Real-time quantification of microRNAs by stem-loop RT-PCR. Nucleic Acids Res 2005;33(20):e179.
[17] Schaffer LG, Tommerup N, ISCN. An International System for Human Cytogenetic Nomenclature. S. Karger; 2005.
[18] van Zutven LJ, Velthuizen SC, Wolvers-Tettero IL, van Dongen JJ, Poulsen TS, MacLeod RA, et al. Two dual-color split signal fluorescence in situ hybridization assays to detect t(5;14) involving HOX11L2 or CSX in T-cell acute lymphoblastic leukemia. Haematologica 2004;89(6):671–8.
[19] Vandesompele J, De Preter K, Pattyn F, Poppe B, Van Roy N, De Paepe A, et al. Accurate normalization of real-time quantitative RT-PCR data by geometric averaging of multiple internal control genes. Genome Biol 2002;3(7) [RESEARCH0034].
[20] Livak KJ, Schmittgen TD. Analysis of relative gene expression data using real-time quantitative PCR and the 2(-Delta Delta C(T)) method. Methods 2001;25(4):402–8.
[21] Chng WJ, Santana-Davila R, Van Wier SA, Ahmann GJ, Jalal SM, Bergsagel PL, et al. Prognostic factors for hyperdiploid-myeloma: effects of chromosome 13 deletions and IgH translocations. Leukemia 2006;20(5):807–13.
[22] Chang H, Bouman D, Boerkoel CF, Stewart AK, Squire JA. Frequent monoallelic loss of D13S319 in multiple myeloma patients shown by interphase fluorescence in situ hybridization. Leukemia 1999;13(1):105–9.
[23] Fassas AB, Spencer T, Sawyer J, Zangari M, Lee CK, Anaissie E, et al. Both hypodiploidy and deletion of chromosome 13 independently confer poor prognosis in multiple myeloma. Br J Haematol 2002;118(4):1041–7.
[24] Kaufmann H, Kromer E, Nosslinger T, Weltermann A, Ackermann J, Reisner R, et al. Both chromosome 13 abnormalities by metaphase cytogenetics and deletion of 13q by interphase FISH only are prognostically relevant in multiple myeloma. Eur J Haematol 2003;71(3):179–83.
[25] Shaughnessy Jr J, Tian E, Sawyer J, McCoy J, Tricot G, Jacobson J, et al. Prognostic impact of cytogenetic and interphase fluorescence in situ hybridization-defined chromosome 13 deletion in multiple myeloma: early results of total therapy II. Br J Haematol 2003;120(1):44–52.
[26] Dewald GW, Therneau T, Larson D, Lee YK, Fink S, Smoley S, et al. Relationship of patient survival and chromosome anomalies detected in metaphase and/or interphase cells at diagnosis of myeloma. Blood 2005;106(10):3553–8.
[27] Chiecchio L, Protheroe RK, Ibrahim AH, Cheung KL, Rudduck C, Dagrada GP, et al. Deletion of chromosome 13 detected by conventional cytogenetics is a critical prognostic factor in myeloma. Leukemia 2006;20(9):1610–7.
[28] Dohner H, Stilgenbauer S, Benner A, Leupolt E, Krober A, Bullinger L, et al. Genomic aberrations and survival in chronic lymphocytic leukemia. N Engl J Med 2000;343(26):1910–6.
[29] Rowntree C, Duke V, Panayiotidis P, Kotsi P, Palmisano GL, Hoffbrand AV, et al. Deletion analysis of chromosome 13q14.3 and characterisation of an alternative splice form of LEU1 in B cell chronic lymphocytic leukemia. Leukemia 2002;16(7):1267–75.
[30] Eis PS, Tam W, Sun L, Chadburn A, Li Z, Gomez MF, et al. Accumulation of miR-155 and BIC RNA in human B cell lymphomas. Proc Natl Acad Sci USA 2005;102(10):3627–32.
[31] Staaf J, Lindgren D, Vallon-Christersson J, Isaksson A, Goransson H, Juliusson G, et al. Segmentation-based detection of allelic imbalance and loss-of-heterozygosity in cancer cells using whole genome SNP arrays. Genome Biol 2008;9(9):R136.
[32] Lai WR, Johnson MD, Kucherlapati R, Park PJ. Comparative analysis of algorithms for identifying amplifications and deletions in array CGH data. Bioinformatics 2005;21(19):3763–70.
[33] Feng S, Liang Q, Kinser RD, Newland K, Guilbaud R. Testing equivalence between two laboratories or two methods using paired-sample analysis and interval hypothesis testing. Anal Bioanal Chem 2006;385(5):975–81.